Weld defect formation in rail thermite welds

Y Chen[1]*, **F V Lawrence**[2], **C P L Barkan**[2], and **J A Dantzig**[3]
[1]Energy Technology Division, Argonne National Laboratory, Argonne, Illinois, USA
[2]Civil and Environmental Engineering Department, University of Illinois at Urbana-Champaign, Urbana, Illinois, USA
[3]Mechanical and Industrial Engineering Department, University of Illinois at Urbana-Champaign, Urbana, Illinois, USA

The manuscript was received on 10 November 2005 and was accepted after revision for publication on 14 June 2006.

DOI: 10.1243/0954409JRRT44

Abstract: A previously developed heat transfer model is used to study the influence of welding parameters on weld defect development in thermite welds. Weld defect formation maps are constructed from a series of heat transfer simulations. For the current normal rail thermite welding conditions, it is found that shrinkage cavity formation can be avoided but cold-lap and centre-line defects are likely to occur. This study also shows that increasing the preheating time or the liquid temperature can suppress the development of cold-lap and centre-line defects but can lead to a slightly higher microporosity content in the railhead as well. Alternatively, it is found that instead of increasing the preheating time or the liquid temperature, the same effect can be achieved by increasing the 25 mm weld gap (standard) to a slightly larger value.

Keywords: rail thermite welding, weld defect, shrinkage cavity, centre-line defect, microporosity

1 INTRODUCTION

Various studies seeking to improve the quality of thermite welds have been conducted over the years. The efforts were mainly focused on alloy hardening [**1**], postweld heat treatments [**2**, **3**], welding procedures [**4**–**6**], and weld toe geometry [**7**, **8**]. A few studies were also carried out to investigate the role of porosity on fatigue performance of thermite welds [**9**, **10**]. It has been recognized that weld defects control the service performance of thermite rail welds, but little research has been carried out to understand the formation mechanisms of thermite weld defects. To the authors' knowledge, there is no previous investigation of the influence of welding parameters on weld defect development in thermite welds. The intention of this paper is to establish correlations between the weld defect formation and thermal conditions of thermite welding using laboratory thermite welds and a heat transfer model that has been introduced in a separate paper [**11**]. To provide a general understanding of the influence of welding parameters, the results of this study are summarized in the form of defect formation maps, which can be used to guide the selection of welding parameters.

**Corresponding author: Former graduate student of University of Illinois at Urbana-Champaign, Energy Technology Division, Argonne National Laboratory, 9700 South cass Avenue, Building 212, G178, Argonne IL 60439, USA. email: yiren_chen@anl.gov*

2 WELD DEFECTS FORMATION AND THE INFLUENCE OF WELDING PARAMETERS

Although all weld defects have a similar effect on weldment fatigue life – increasing local stress and thus reducing weldment fatigue life – their origins during thermite welding can be quite dissimilar. Some weld defects are caused by foreign objects (slag) in thermite weld metal or by the improper mating between the weld mould and the rail surface. These weld defects are not sensitive to thermal conditions during welding, and are beyond the scope of this study. Previous researches by Schroeder and Poirier [**4**], Cyre [**7**], and Ross [**8**] provide insights about the formation of these defects. This paper focuses on four weld defects (cold-lap, shrinkage cavity, centre-line defect cluster, and microporosity) whose formation mechanisms have a strong thermal basis. Using both laboratory thermite welds and thermal analyses, the formation conditions of these weld

defects will be identified, and the influence of welding parameters on their formation will be analysed.

2.1 Cold-lap defect

2.1.1 The criterion for cold-lap formation

Cold-laps can often be found at weld toes in the rail base and are caused by inadequate fusion between weld metal and the surface of rail ends. Figure 1(a) shows a cold-lap defect in a laboratory thermite weld. The possible severe consequence of cold-lap defect is evident in the micrograph that shows a fatigue microcrack emerging from the root of cold-lap defect in a thermite weld which has been fatigue cycled.

Unlike the inadequate fusion caused by the improper mating between weld mould and rail surface, cold-lap defects can occur even at the locations where the weld mould is properly fitted to the rail surface. Figure 1(b) is a sketch that illustrates the formation of cold-lap defect during solidification. The side view of a thermite weld setup shows that the rail end passes beyond the mould collar and sticks out into the weld mould. This part of the rail end is called a 'stick-out', and it is exposed to the molten metal when liquid steel is introduced into the weld cavity. The dashed lines in Fig. 1(b) represent the original profile of rail ends. After encountering the liquid metal, a certain volume of rail end melts, and the solid–liquid interface moves into the rail. The depth of the rail end penetrated by the liquid metal is defined as 'melt-back'. If the melt-back depth is smaller than stick-out, a small triangle-shaped liquid metal is formed underneath the rail base, as shown in Fig. 1(b). This portion of liquid metal is subject to the strong mould cooling and the heat flow direction is mainly from weld metal towards mould. Thus, the penetration by liquid metal into the stick-out surface is minimum, and the weld toe area solidifies quickly after pouring. If there is any contamination on the stick-out surface, an inadequate fusion (cold-lap) can occur. In Contrast, if the melt-back is deeper than stick-out, the direction of heat flow will be mainly from the rail centre towards the rail, and the inadequate fusion is unlikely to occur. On the basis of this mechanism, the melt-back depth can be used as a parameter to characterize the likelihood of the cold-lap formation. The assumed condition for cold-lap to develop is that the melt-back depth must be less than the stick-out.

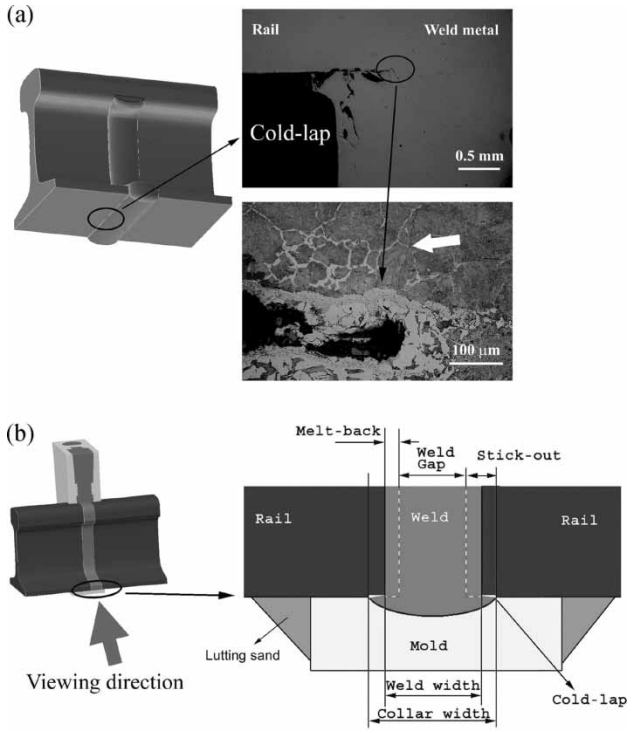

Fig. 1 (a) A cold-lap defect in rail base, and (b) a schematic illustration of cold-lap defect formation

2.1.2 The influence of welding conditions on cold-lap defect formation

A series of simulations were conducted using the heat transfer model described in reference [**11**]. The geometry of the heat transfer model is based on an SkV* standard thermit weld and a 136 lb/yard rail. Three weld gap dimensions, 25, 38, and 50 mm, were used in this study. The weld mould collar width is 39.4 mm for a 25 mm weld gap, 52.1 mm for a 38 mm weld gap, and 64.8 mm for a 50 mm weld gap. The average heat-input profile obtained from laboratory thermite welds in reference [**11**] was applied to the rail end during the preheating stage. A 60 s tapping time (time period between the end of preheating and the beginning of solidification) and a homogenous liquid temperature distribution in the welding pool were assumed for this set of simulations. The welding parameters and their range examined in these simulations are summarized in Table 1.

The solidus isotherms at 1 mm underneath the rail base surface were plotted at different times. The furthest isothermal line away from the original rail end was considered to be the line of fusion. The melt-back depth (d) was measured from the line of fusion to the original rail end, and this stick-out depth was considered as the critical melt-back depth (d_c) to avoid the cold-lap formation.

**A short preheating time thermite welding procedure developed by Orgo-Thermit®.* All common rail steel qualities can be welded with this procedure. The specified preheating time for SkV process varies from 1.5 to 7 min depending on the rail section.

Table 1 Welding parameters considered for cold-lap formation

Welding parameters	Range
Liquid temperature (°C)	1800–2200
Preheating time (min)	0–7
Weld gap (mm)	25–50
Stick-out distance (mm)	3–9

2.1.2.1 The influence of preheating time and liquid temperature. Figure 2(a) shows the simulation results for a 25 mm weld gap and a 7 mm stick-out. The critical value of d_c is shown as a horizontal dashed line in the figure. Above this line, the liquid temperature would avoid the cold-lap formation. Below it, a cold-lap is likely to form. From Fig. 2(a), it can be seen that with an increase in preheating time, the melt-back depth increases. For the 2200 and 2000 °C liquid temperatures, the critical preheating times are 2.5 and 4.7 min, respectively. For the 1800 °C liquid temperature, the critical preheating time is >7 min.

Similarly, an increase in liquid temperature can also promote rail end melting, and therefore reduce the likelihood of cold-lap formation. Figure. 2(a) shows that if the liquid temperature is increased a shorter preheating time is needed to produce a sufficient melt-back. Figure 2(b) further illustrates the critical values of liquid temperature. For 5 and 7 min preheating, the minimum requirements on liquid temperatures are ~1980 and 1880 °C, respectively. For 0 and 2 min preheating, the minimum liquid temperatures are >2200 °C.

2.1.2.2 The influence of weld gap and stick-out dimensions. The melt-back depth does not vary substantially with weld gap width. Figure 2(c) shows that the variation of melt-back depth with weld gap is very small. Only for the high liquid temperature can a slight increase in rail end melt-back be seen. This rather weak dependence of melt-back on weld gap is due to the latent heat absorption by the melted rail end. The position of melting front is determined by the balance between the heat transfer into and out of the melt zone. In a short period of

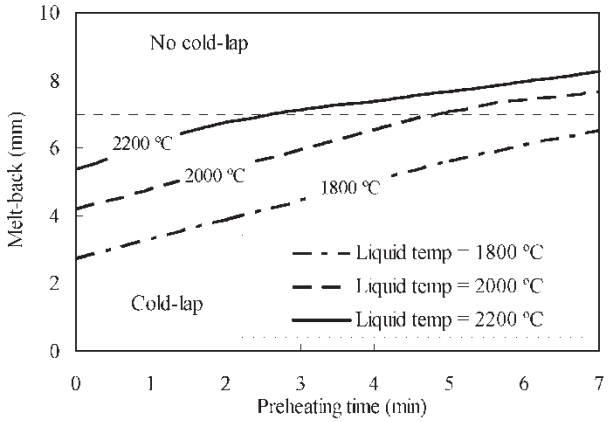

(a) weld gap =25 mm, stick-out=7mm

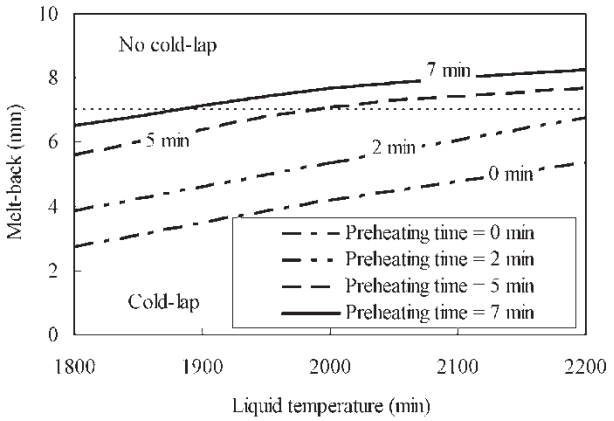

(b) weld gap =25 mm, stick-out=7mm

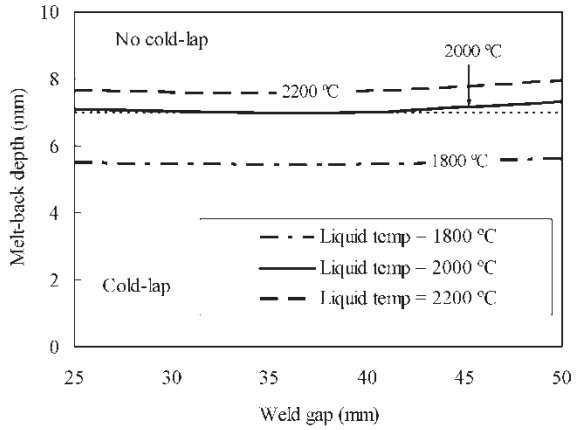

(c) preheating time –5 min, stick-out–7mm

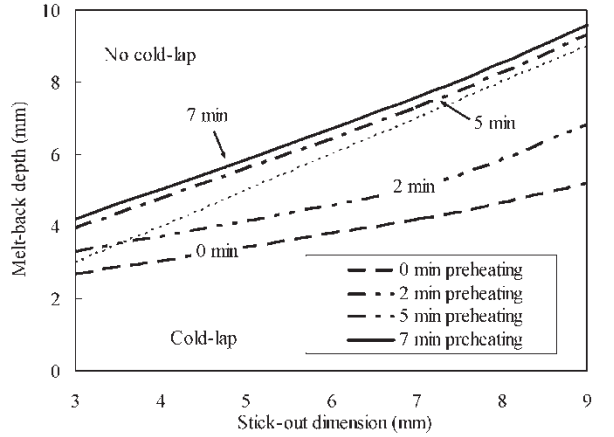

(d) liquid temp. =2000 °C, weld gap=25mm

Fig. 2 The influence of welding parameters on melt-back depth (a) preheating time, (b) liquid temperature, (c) weld gap, and (d) stick-out dimension

time, a wider weld gap cannot alter the temperature gradient significantly in the rail. For this reason, the weld gap has a weak influence on cold-lap formation.

Besides the weld gap, another geometrical parameter that could be changed during thermite welding is the stick-out. By increasing the stick-out, more rail surface area is exposed to the liquid metal; therefore, the melt-back depth increases. However, this increase in melt-back depth (d) does not prevent cold-lap formation because the critical melt-back depth (d_c) increases as well. Figure 2(d) shows that the rate of d_c increase with stick-out exceeds that of d. This means the larger melt-back depth produced by increasing the stick-out dimension does not help prevent cold-lap formation at all. Conversely, a smaller stick-out is more favourable for cold-lap avoidance. By reducing the stick-out dimension, the minimum requirements on both preheating time and liquid temperature to avoid cold-lap formation can be much reduced.

2.2 Shrinkage cavity

2.2.1 The criterion for shrinkage cavity formation

Shrinkage cavity is another serious weld defect and is often found in the rail web area of thermite welds. Figure 3 shows a shrinkage cavity and its formation mechanism in the rail web area. Owing to thermal expansion and phase transformations, the volume of weld metal changes constantly during cooling. The thermal expansion coefficient of liquid metal is significantly higher than that of solid metal. Therefore, the volume reduction of weld metal during cooling is greater in the high-temperature region than in the low-temperature region. At the freezing point, a small additional volume contraction also occurs in the weld metal because of a microstructure change. The volume shrinkage caused by both the phase transformation and temperature reduction leads to a contraction force inside the weld metal. If, at the final stage of solidification, a portion of liquid metal is surrounded by the already solidified material, no additional liquid will flow into this region to compensate for the volume reduction (Fig. 3(b)). Consequently, the force of contraction can cause a shrinkage cavity to form in the weld. Therefore, the development of an isolated liquid region at the final stage of solidification is the critical condition for shrinkage cavity formation.

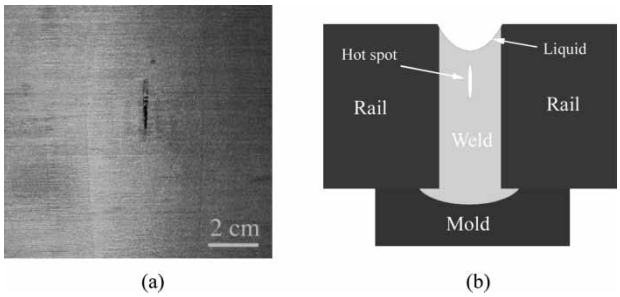

Fig. 3 (a) Shrinkage cavity in the rail web of a laboratory thermite weld, and (b) schematic illustration of the shrinkage cavity formation

2.2.2 The influence of welding conditions on shrinkage cavity formation

A series of thermal simulations were carried out to study the influence of three welding parameters: preheating time, average liquid temperature, and weld gap. In these simulations, the stick-out dimension was fixed to be 7 mm, and upward liquid temperature profiles (liquid temperature increases from rail base towards railhead) were assumed. All the other welding parameters were the same as those specified in section 2.1. For each simulation, the position of solidification front was plotted at different time steps as a series of snapshots to visualize the solidification process inside weld cavity. The presence of an isolated liquid region at the rail web area during solidification was used to determine whether a shrinkage cavity would occur.

Figure 4 shows two simulations with the same average liquid temperature (2050 °C) and weld gap (25 mm); only preheating time is different. Three temperature regions ($T <$ solidus, solidus $< T <$ liquidus, $T >$ liquidus) in the weld metal are distinguished by different shades. During solidification, the solid–liquid interface moves from the rail end towards the weld centre and from the rail base towards the railhead. The liquidus isothermal surface sweeps through the weld section first, whereas the solidus isothermal surface lags behind. For Fig. 4(a), the preheating time is 2 min. When the solidus surface moves past the weld cross-section, an

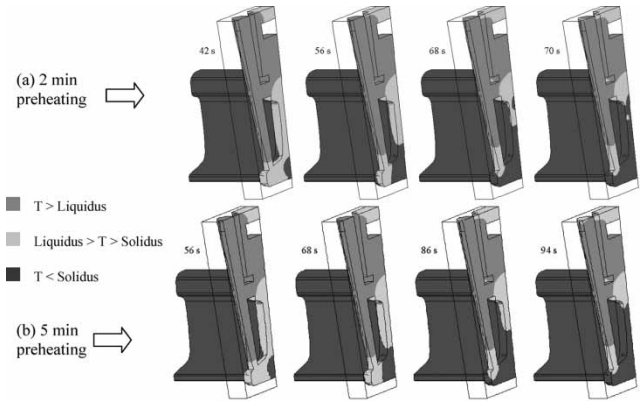

Fig. 4 The influence of preheating time on shrinkage cavity formation (average liquid temperature = 2050 °C, weld gap = 25 mm)

isolated liquid region (lightly shaded spot) appears in the rail web. If the preheating time is increased to 5 min (Fig. 4(b)), the isolated liquid region disappears in the simulation result. This comparison shows that the increase in preheating time is helpful to avoid the development of shrinkage cavity in thermite welds.

Similar simulations were also performed with different liquid temperatures (1900 and 2150 °C) whereas all the other welding parameters were held constant. Snapshots similar to Fig. 4 were generated to determine if an isolated liquid region is present during solidification. The results show that a lower liquid temperature (1900 °C) causes the close of the liquid feeding path much sooner, and an isolated liquid region appears in the case of 5 min preheating time. However, for a higher liquid temperature (2150 °C), no isolated liquid region is found, even without preheating. Hence, increasing liquid temperature can also help prevent the shrinkage cavity formation.

The effect of weld gap on the development of an isolated liquid region is similar to that of liquid temperature. With a larger weld gap (38 or 50 mm), no isolated liquid region is found in the simulations for 2050 °C liquid temperature and no preheating. For the simulations with 1900 °C liquid temperature, an isolated liquid region is present if the weld gap is 38 mm but disappears when the weld gap is increased to 50 mm. It is obvious that a larger weld gap helps eliminate the development of shrinkage cavity, and can reduce the minimum requirements on the preheating time and the average liquid temperature significantly.

To summarize the influence of welding conditions on shrinkage cavity formation, a higher liquid temperature, a longer preheating time, and a wider weld gap can all promote the vertical motion of solidification front and suppress the horizontal motion of solidification front in the weld centre; therefore, can help prevent the development of shrinkage cavities in thermite welds.

2.3 Centre-line defect

2.3.1 The criterion for centre-line defect formation

Weld defects can be seen along with the weld centre-line in radiographs of thermite welds (Fig. 5(a)). The optical micrograph of this defective region (Fig. 5(b)) reveals that these centre-line defects are accumulation of shrinkage type defects, which are much smaller than the macroscopic shrinkage cavity discussed in section 2.2. It is also found that the centre-line defect is more pronounced in the rail web and is less severe in the rail base. No centre-line defect was found in the railhead region in laboratory thermite welds.

Similar to the shrinkage cavity, the formation of a centre-line defect cluster is caused by the volumetric shrinkage and the liquid pressure drop in the mushy zone during solidification. However, unlike the shrinkage cavity formation, no macroscopic isolated liquid region during solidification is required for centre-line defect to occur. The pressure drop caused by liquid flow through the dendrite structure, with the assistance of gas evolution during solidification, is sufficient to allow the centre-line defect cluster to develop [**12**]. In foundry practice, it has been long recognized that the local temperature gradient (G), cooling rate (R), and solidification rate (V) are all important to produce this type of defect [**13**]. Many studies have been conducted to relate these thermal parameters with centre-line defect formation [**14–16**]. The correlations obtained are mostly empirical and have had various degrees of success in different materials. Among them, Niyama's modified temperature gradient criterion has been proven for the steel castings, especially for predicting the shrinkage pores along with casting centre-line. In reference [**17**], Niyama *et al.* showed that the ratio of temperature gradient and the square root of cooling rate can be used to predict the shrinkage pores at the centre of a casting. On the basis of their experimental results for low carbon steel casting, they showed that a critical value of $G/\sqrt{R} = 1\ ^{\circ}\mathrm{C}^{1/2}\,\mathrm{min}^{1/2}/\mathrm{cm}$ correlated well with the appearance of shrinkage pores along the casting centre-line. Below this critical value, porosity developed in their casting, and above this value, shrinkage pores were unlikely. Darcy's law was used to justify the correlation between the formation of centre-line defect and Niyama's parameter $G/\sqrt{R}$. Because of the success of Niyama's modified temperature gradient in predicting shrinkage pores, this model was selected to determine the centre-line defect formation in the study.

As an empirical criterion, the critical value of the Niyama's modified temperature gradient is material sensitive and needs to be determined for thermite steel. From the simulations of laboratory welds, the temperature gradient and local cooling rate at 1 and 10 mm away from the latitudinal weld centre

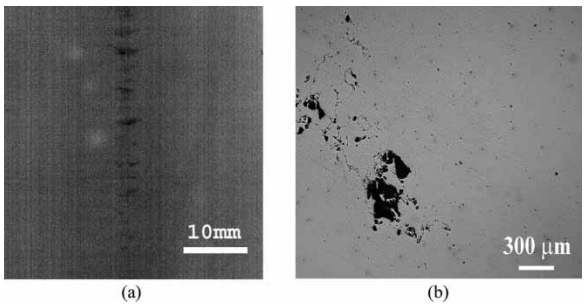

Fig. 5 (a) X-ray radiograph image and (b) optical micrograph of defect cluster along weld centre-line

in railhead, web, and base were extracted at solidus temperature, and then the modified temperature gradient ($G/\sqrt{R}$) was calculated for each examined location. The graphic representation of Niyama's analysis is given in Fig. 6, where the temperature gradients are plotted against the cooling rates for all locations examined in the laboratory welds. The data points fall into two separate groups: one group is at the upper left corner where the shrinkage porosity is not possible, and another group is at the lower right corner where the shrinkage cavity is expected. The constant $G/\sqrt{R}$ values appear as parallel lines in Fig. 6. The line of $G/\sqrt{R} = 2\ ^{\circ}\mathrm{C}^{1/2}\,\mathrm{min}^{1/2}/\mathrm{cm}$ passes through the intermediate of no defect and defect region and therefore, is selected as the critical value to determine the formation of centre-line defect in thermite welds.

2.3.2 *The influence of welding conditions on centre-line defect formation*

In order to study the influence of welding parameters on the centre-line defect formation, a series of thermal simulations were performed. Three welding parameters (liquid temperature, weld gap, and preheating time) were explored in these simulations. The temperature gradient and cooling rate were evaluated at the solidus temperature for each simulation. The calculated G and R are plotted in Fig. 7, and the centre-line defect region is separated from the no-centre-line-defect region by a straight line of $G/R^{1/2} = 2\ (^{\circ}\mathrm{C}^{1/2}\,\mathrm{min}^{1/2}/\mathrm{cm})$. The arrows in Fig. 7 represent the increase direction of the indicated welding parameters. Figure 7(a) shows the effect of average liquid temperature. It can be seen that the liquid temperature does not have a significant impact on the centre-line defect formation. With the increase in the liquid temperature, R decreases and G remains the same. Therefore, Niyama's parameter ($G/R^{1/2}$) is basically unchanged. The welding condition moves nearly parallel to the constant $G/R^{1/2}$ line with the increase in liquid temperature. Similarly, the increase in preheating time does not have a strong effect on Niyama's parameter either (Fig. 7(c)). With the increase in preheating time, the welding condition remains in the same side of the G–R plot for all locations in a thermite weld. The most influential welding parameter for the centre-line defect formation is weld gap (Fig. 7(b)). With the increase in weld gap from 25 to 38 mm, R is decreased, but at the same time, G at rail base and web is increased considerably. It can be seen that the welding condition in the rail base and rail web moves towards the upper left corner and enter the no-defect zone. A further increase in weld gap from 38 to 50 mm does not lead to an additional improvement in terms of avoiding centre-line defect formation; instead, a small decrease in Niyama's parameter is observed when the weld gap increases from 38 to 50 mm.

2.4 Distributed microporosity

Distributed microporosity refers to the uniformly distributed small pores often observed in weld metal. The size of micropores varies from a few to nearly a hundred microns. Both spherical and irregularly shaped micropores can be found, and they are

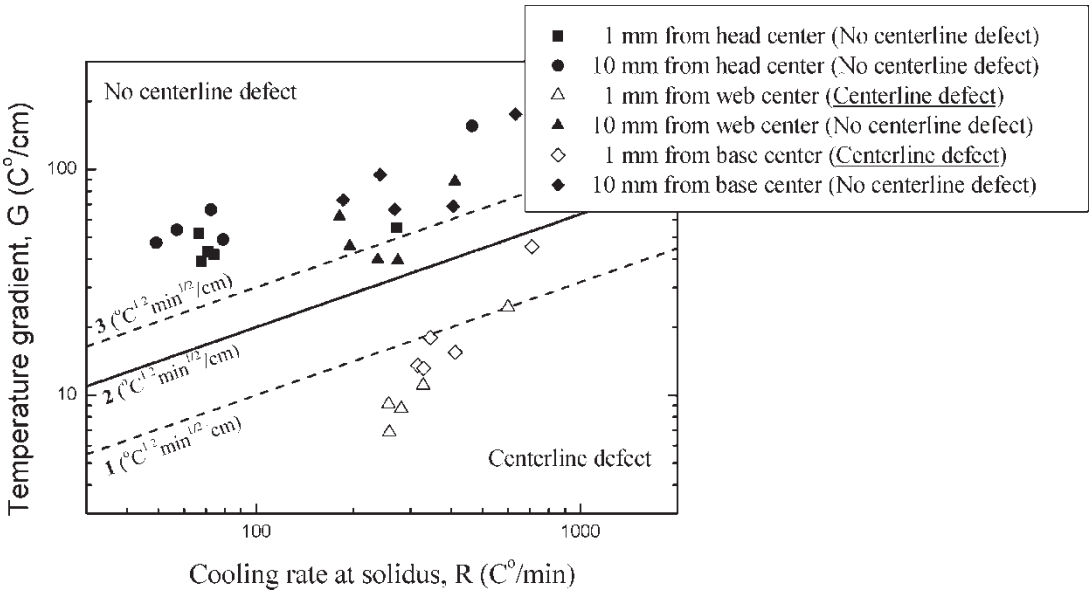

Fig. 6 Niyama's temperature gradient criterion of centre-line defect formation (the experimental observations are given in the parentheses in the legend)

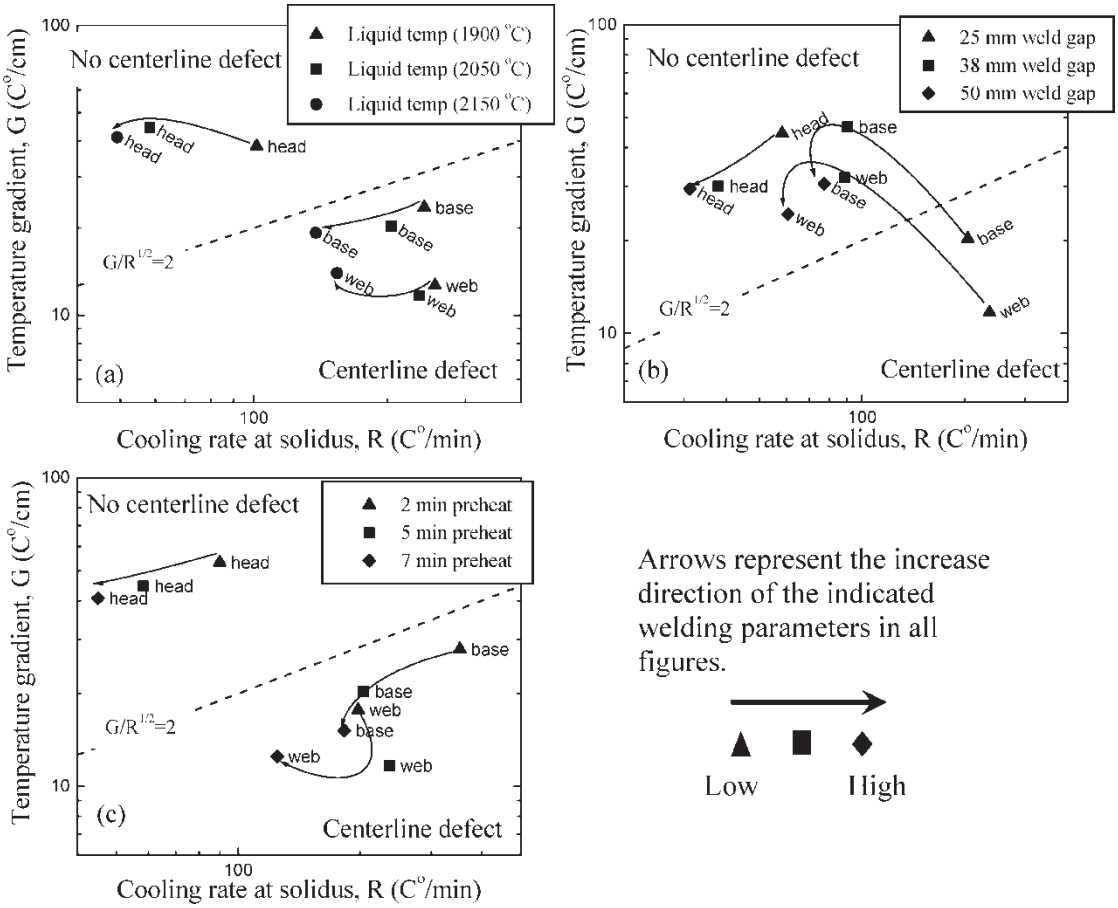

Fig. 7 The influence of various welding parameters on centre-line defect formation (a) effect of liquid temperature, (b) effect of weld gap, and (c) effect of preheating time

usually located in the interdendrite regions as shown in Fig. 8.

The formation of microporosity involves both gas evolution during cooling and the liquid pressure drop inside the mushy zone (temperature between the solidus and liquidus). In a comprehensive analysis of the interdendrite porosity in Al–Cu alloy containing hydrogen, Poirier *et al.* [**18**] demonstrated that the formation condition of an interdendrite pore is

$$P_G - P_L = \frac{4\gamma}{f_L \lambda_1} \tag{1}$$

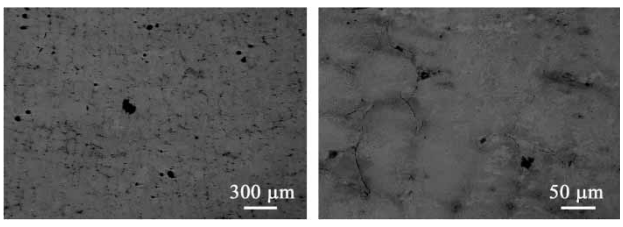

Fig. 8 Spherical and irregular shape micropores in the interdendrite regions

where P_G is the gas pressure inside the pore, P_L the liquid pressure within the mushy zone, γ the surface tension between gas and liquid, f_L the volume fraction of interdendritic liquid, and λ_1 the primary dendrite arm spacing. It can be seen that the larger the dendrite arm spacing, the easier the interdendrite pores will develop. By further assuming that the gas phase comprises the supersaturated gas of liquid- and of solid-phase, Poirier showed the volume fraction of interdendrite pores is a decreasing function of the gas pressure inside pores (P_G^E) at the eutectic temperature [**18**]

$$\text{Vol\%} = \left\{1 + \left(\frac{1 - f_E}{\rho_s'} + \frac{f_E}{\rho_{LE}}\right)\frac{MP_G^E}{RT_E\phi}\right\}^{-1} \tag{2}$$

where f_E is the eutectic fraction, ρ_s' and ρ_{LE} the mass densities of solid and liquid eutectic at the eutectic temperature, M molecular weight of gas, R the gas constant, T_E the eutectic temperature, and ϕ the fraction of gas-phase in alloy at eutectic temperature. As the required gas pressure to form interdendrite pores decreases with dendrite arm spacing, the volume percentage of pores increases with dendrite arm

spacing, i.e. the larger the dendrite arm spacing, the higher the fraction of porosity.

To obtain a correlation between the microporosity and thermite welding condition, the dependence of dendrite arm spacing on solidification condition is needed. According to Kurz and Fisher [**19**], the primary dendrite arm spacing decreases with the increasing temperature gradient and solidification rate (V), and can be described by

$$\lambda_1 \propto G^{-0.5} V^{-0.25} \tag{3}$$

Therefore, the volume fraction of microporosity can be correlated to the thermal condition during solidification for thermite welds.

In the light of this analysis, the correlation between the volume fraction of microporosity and thermal conditions was examined in our laboratory thermite welds. First, heat transfer simulations were performed with the welding condition identical to the laboratory welds. Then, the temperature gradient and solidification rate were calculated at different locations. Consequently, the volume fraction of microporosity measured at the same locations was plotted against the dendrite arm spacing parameter, $G^{-0.5}V^{-0.25}$, as shown in Fig. 9. The increasing trend of microporosity content with dendrite arm spacing is evident. However, owing to the scatter in the microporosity measurements, the correlation between the microporosity content and $G^{-0.5}V^{-0.25}$ appears as a band. Thus, a quantitative estimate of the microporosity content based on the thermal variables is difficult in thermite welds. Nonetheless, it can still safely be concluded that, with a decrease in the temperature gradient and solidification rate, more distributed microporosity is expected in thermite welds. Within the range of welding condition used in laboratory welds, the increasing trend of volume fraction of porosity with parameter $G^{-0.5}V^{-0.25}$ is linear, and a curve fit for the data in Fig. 9 provides the relation to predict severity of microporosity in thermite welds: vol% $= 0.18 + 1.32(G^{-0.5}V^{-0.25})$.

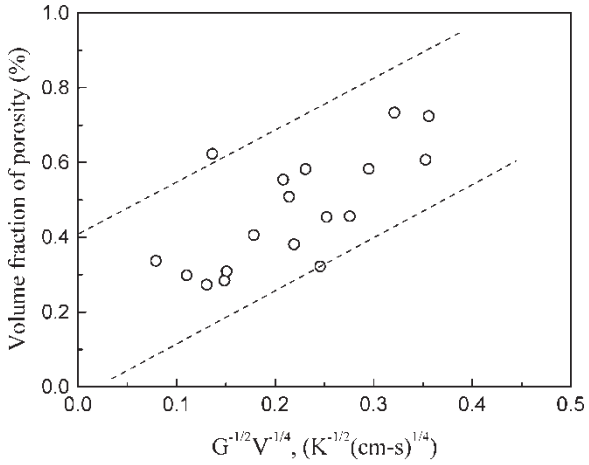

Fig. 9 Volume percentage of microporosity in laboratory thermite welds versus thermal parameter $G^{-0.5}V^{-0.25}$

3 WELD DEFECT FORMATION MAPS

To improve the quality of thermite rail welds, the welding parameters need to be optimized so that the occurrence and severity of weld defects are minimized. It is useful to have general maps which show the values of the welding parameters that cause the formation of weld defects. In this section, the critical conditions for several weld defects considered in this study are utilized to construct 'defect formation maps'. On the basis of these maps, strategies to improve the reliability of rail thermite welds will be suggested.

3.1 Welding parameters and weld defects considered

The focus is only on three welding parameters that have a strong influence on weld defect development and can be controlled in practice: the weld gap, the liquid temperature, and the preheating time. A 7 mm stick-out dimension and 60 s tapping time were assumed for all calculations in this section.

Four weld defects whose formation mechanisms have been dealt with in previous sections are considered here: cold-lap in rail base, shrinkage cavity in rail web, centre-line defect cluster in rail base and web, and microporosity in rail head. Although microporosity can also be found in places other than the railhead, the presence of these microdiscontinuities does not affect fatigue crack growth significantly as shown by Carpenter *et al.* [**20**] and Barsom and Imh of [**21**]. Only in the area where more severe weld defects are absent, such as in the railhead do the micropores develop the critical fatigue cracks [**15**]. For this reason, only the microporosity in the railhead is considered.

3.2 Weld defect formation maps

On the basis of the analyses in section 2, the following characteristic parameters and their critical values were used to describe the formation or severity of weld defects.

1. *For cold-lap formation*. The melt-back depth is used to characterize the occurrence of cold-lap.

When the melt-back is <7 mm stick-out, a cold-lap is assumed to occur.

2. *For shrinkage cavity formation*. The presence of an isolated liquid region during solidification is considered as a signal of shrinkage cavity formation. The value of welding parameter between two subsequent simulations (with only one welding valuable altered) is assumed to be the critical condition for shrinkage cavity formation.
3. *For centre-line defect cluster formation*. Niyama's modified temperature gradient ($G/R^{1/2}$) is used to define centre-line defect formation. $G/\sqrt{R} = 2$ ($^{\circ}C^{1/2}$ $min^{1/2}$/cm) is assumed to be the critical condition for the formation of a centre-line defect.
4. *For microporosity severity*. Microporosity is inevitable in thermite rail welds. Thus, instead of determining the criterion for microporosity formation, the severity of microporosity is described. A linear fit to the experimental data in Fig. 9, $\text{vol\%} = 0.18 + 1.32(G^{-0.5}V^{-0.25})$, serves as the correlation between the welding parameters and the severity of microporosity.

These characteristic parameters are calculated from the simulation results, and their critical values are plotted in different welding parameter spaces. Figure 10 shows the obtained defect formation maps. The iso-parametric lines in the figures are volume percentage of microporosity in the railhead.

In defect formation maps, the shrinkage cavity region and cold-lap region have the similar shape and are both located at the lower left corner. The cold-lap defect is more likely to form compared to the shrinkage cavity. The shape of centre-line defect region is more complicated and located at the lower part of defect formation maps in Figs 10(a) to (d). Between the rail web and rail base, the centre-line line defect is more likely to occur in the rail web. It is easier to avoid the centre-line defect formation in the rail web with an intermediate liquid temperature or preheating time. A generally increasing trend from lower left to upper right can be seen for the microporosity volume fraction in all defect formation maps. The microporosity content is expected to be the highest in the region where all the other defects are absent as shown in Figs 10(a) to (d).

4 DISCUSSION

4.1 Limitations of the defect formation maps

The defect formation maps show that cold-lap defects can occur for a wide range of welding parameters; however, in both the laboratory and field thermite welds, cold-lap defects were not very often observed. There may be two reasons for this contradiction. First, the cold-lap defect is similar to the fin defect which is an inadequate fusion defect caused by improper mating between the weld mould and rail surface [**8**]. It is difficult to differentiate a cold-lap from a fin defect in practice. Second, the predicted onset of cold-lap formation in the analysis is based on the assumption that the weld gap width is precisely the distance between two butted rail ends. Given the fixed weld mould collar width, the dimension of the stick-out is certain. In the simulations, the dimension of stick-out is assumed to be exactly 7 mm. However, in actual thermite welding, the weld gap is prepared by placing a solid gauge block (25 mm for a standard thermite weld) between two rail ends. It is unlikely that the weld gap could be smaller than the width of the gauge block; instead, it is possible that the actual weld gap would be larger (so the gauge block can be removed prior to the mould installation). As a result, the stick-out distance might normally be smaller than 7 mm, and the cold-lap formation would thus become less likely. If only 5 or 6 mm of horizontal melting of the rail end is needed, the boundary of the cold-lap formation region would move considerably towards the left in a defect formation map. Therefore, these maps obtained using the assumption of a 7 mm stick-out distance may overstate the possibility of cold-lap formation in thermite welds.

The accuracy of defect formation maps depends not only on the precision of the thermal simulations but also upon the density of the simulations performed. When traversing through the welding parameter space, the smaller the increments used, the more accurately the regions of weld defect formation can be determined. This is especially true for the critical condition of shrinkage cavity. To construct the defect formation maps, three simulations were performed for each welding parameter. These big increments may affect the precision of the shrinkage cavity formation region. To accurately determine when a shrinkage cavity may occur, many more simulations using finer increments of the welding variables are needed.

The microporosity content was estimated based on a linear correlation between the calculated dendrite arm spacing ($G^{-1/2}V^{-1/4}$) and the measured porosity content (Fig. 9). In fact, the volume fraction of microporosity is a complex function of the primary dendrite arm spacing, and becomes saturated at larger dendrite arm spacing [**18**]. The linear correlation used to calculate the microporosity content is over simplified. For this reason, the variations of porosity content shown in the defect formation maps can only be treated as trends. The actual volume percentage of porosity in a thermite weld may be different.

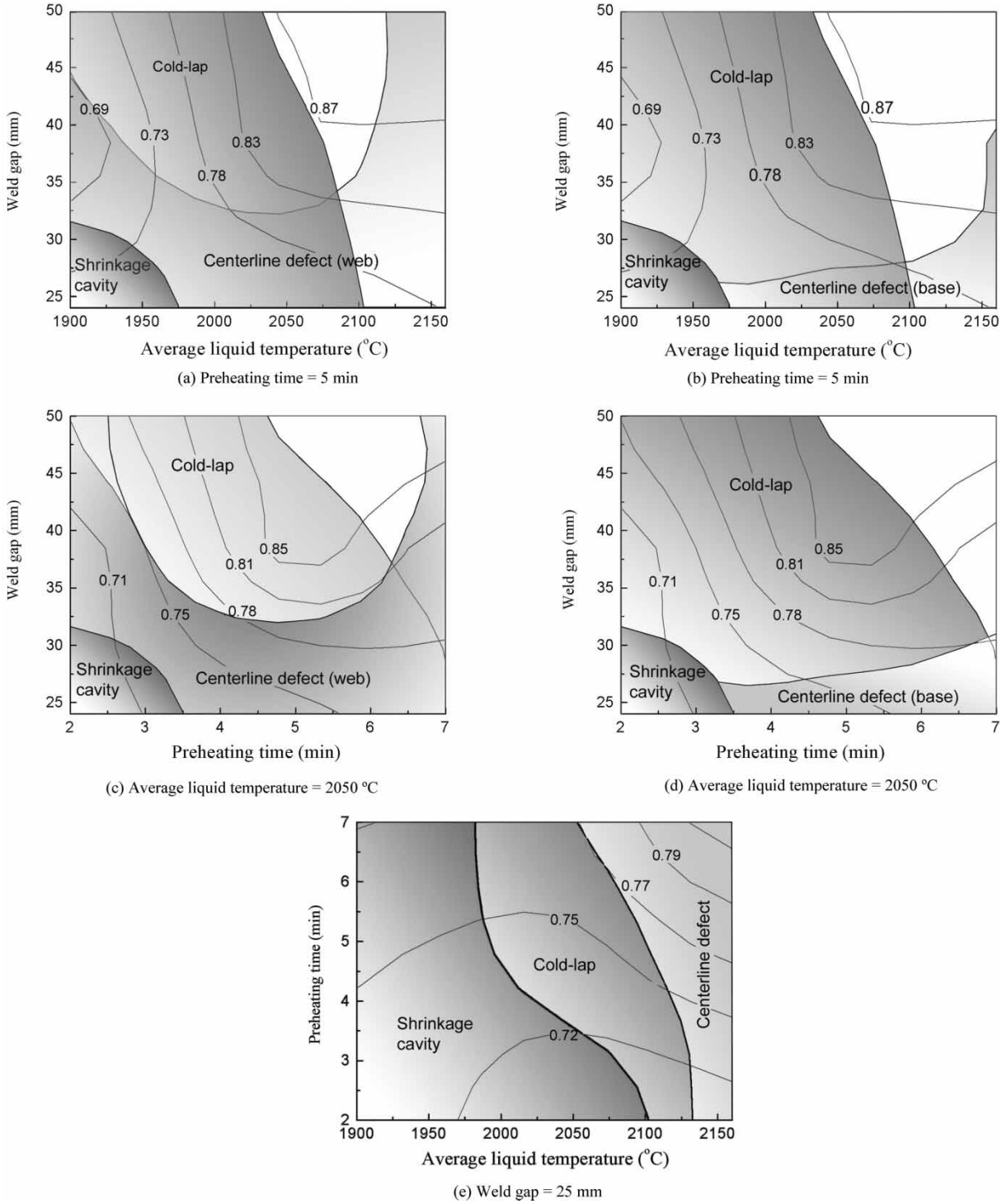

Fig. 10 Weld defect maps in different welding parameter spaces. The iso-parametric lines are the volume percentage of microporosity in the railhead (vol%). Centre-line defect is examined in the rail web for (a) and (c), and in the rail base for (b) and (d). In the case of (e), the area of centre-line defect formation is the same in both the rail web and base

4.2 Suppressing the weld defects in thermite welds

Weld defect regions overlap and cover different ranges of welding parameters in defect formation maps. Among these defect areas, the cold-lap defect and the shrinkage cavity have a similar shape; they are both located at the lower left corner of the defect formation maps. Increasing the liquid temperature, preheating time, and weld gap can

help eliminate the cold-lap and the shrinkage cavity. To eliminate the cold-lap, increasing the liquid temperature and the preheating time is more effective. In contrast, increasing the liquid temperature and weld gap is more effective in eliminating the shrinkage cavity. The boundary for shrinkage cavity formation is further left and lower than that of cold-lap in all defect maps. Thus, with a welding condition that can eliminate cold-lap, the formation of shrinkage cavities can also be avoided, but getting rid of cold-lap defects would require a larger increase in the welding parameters. If the stick-out of the rail end is smaller ($<$7 mm for the standard thermite weld), the critical conditions for cold-lap elimination may not be very different from that for shrinkage cavity removal.

The welding conditions for suppressing the centre-line defect formation are more complicated. For the rail web, the centre-line defect does not occur in the mid-range of welding parameters (Figs 10(a) and (c)). However for the rail base, the formation of centre-line defect appears strongly dependent on the weld gap and weakly dependent on the liquid temperature and preheating time in most areas (Figs 10(b) and (d)). In the defect formation maps, the boundary for centre-line defect formation in the rail web occurs at a larger weld gap than in the rail base. Therefore, if the weld gap is increased to eliminate the centre-line defect in the rail web, any centre-line defect in the rail base is likely to be suppressed as well. A small increase in the preheating time and liquid temperature will reduce the occurrence of the centre-line defect in the rail web; but beyond certain values, further increases in the preheating time and liquid temperature will increase the tendency for centre-line defect formation. This transition point is at $\sim$2050 °C for liquid temperature and 5 min for preheating time. The increases in preheating time and liquid temperature will not affect the centre-line defect formation in the rail base significantly, unless the liquid temperature is very high.

The formation of microporosity is inevitable in thermite welds, at least in the ranges of welding parameters considered in this study. The dependence of microporosity content on the welding parameters is opposite to that of the cold-lap and shrinkage cavity. The higher the liquid temperature and the wider the weld gap, the higher volume percentage of microporosity. Hence, the elimination of cold-lap defects, shrinkage cavities and centre-line defects will be achieved at the price of increasing the microporosity content. Fortunately, this increase is not significant.

If the microporosity in thermite welds is ignored, it is possible to produce thermite welds without weld defects (free from cold-lap, shrinkage cavity, and centre-line defects) according to Figs 10(a) to (d). The current standard thermite welding conditions are 25 mm weld gap, 5 min preheating time*, and 2050 °C average liquid temperature. To produce such a 'no defect' thermite weld (microporosity would still exist), the preheating time is kept unchanged and the liquid temperature is increased to $\sim$2100 °C and the weld gap to 35 mm; or the liquid temperature is kept unchanged and the preheating time is increased to $\sim$6.25 min and the weld gap to 38 mm. In both cases, the weld gap is increased considerably, and varying the liquid temperature or preheating time alone cannot produce a satisfactory result.

5 CONCLUSIONS

1. With the current standard rail thermite welding practice, shrinkage cavities can be avoided, but cold-lap and centre-line defect formation is likely. With increasing preheating time and liquid temperature, the likelihood of cold-lap and centre-line defect formation is reduced.
2. Microporosity cannot be eliminated in thermite welds. The welding conditions that are favourable for avoiding cold-lap and centre-line defects (increasing the preheating time and liquid temperature) are likely to lead to a larger amounts of microporosity.
3. Increasing the weld gap dimension helps avoid the cold-lap and centre-line defect formation. In fact, to eliminate cold-lap and centre-line defects in thermite welds, the current standard 25 mm weld gap should be increased. Increasing either the preheating time or the liquid temperature individually is not as effective as increasing the weld gap. With the current standard thermite welding process, a 38 mm weld gap with a slight increase in preheating time will be the most practical approach to obtain thermite welds free from major weld defects.

ACKNOWLEDGEMENTS

The authors would like to thank Joseph Kristan and David Davis of the Association of American Railroads' Transportation Technology Center Inc. and Frik Hefer of Orgo-Thermit Inc. for their interesting discussions throughout this study. Dr Grzegorz Banas, Eric Ross, Jeff Cyre, and Alberto Alvarez-Lozano from University of Illinois at Urbana-Champaign are also

It is assumed that the preheating heat flux is the same in all cases, so the preheating time can truly represent the preheating result.

acknowledged for their contributions to the experimental effort. This work was sponsored by the Association of American Railroads Technology Scanning and Strategic Research Programs and the Transportation Research Board High Speed Rail IDEA Program (HSR-41). The computational work was partially supported by National Computational Science Alliance under MSS030005N and utilized the IBM P690.

REFERENCES

1 **Schroeder, L. C.** and **Poirier, D. R.** The mechanical properties of thermite welds in premium alloy rails. *Mater. Sci. Eng.*, 1984, **63**, 1–21.
2 **Jha, B.** *Thermite welding of rail steel*. PhD Dissertation, Illinois Institute of Technology, 1989.
3 **Nenad, I., Jovanovic, M. T., Todorovic, M., Trtanj, M.,** and **Saponjic, P.** Microstructural and mechanical characterization of postweld heat-treated thermite weld in rails. *Mater. Charact.*, 1999, **43**, 243.
4 **Schroeder, L. C.** and **Poirier, D. R.** Thermite Rail welds, the process, mechanical and metallurgical properties, and possible improvements. Proceedings of Railroad Rail Welding, Memphis, 29–30 November 1983, p. 21.
5 **Fry, G. T.** *A modified thermite rail welding procedure*. MS Thesis, University of Illinois at Urbana-Champaign, 1992.
6 **Gianetto, J. A., Es-Sadiqi, E., Sawley, K. J., Joos, M. A.,** and **Blowatt, D. W.** Influence of EMS on rail thermite weld structure and properties. Proceedings of the *39th mechanical working and steel processing conference-international symposium on rail steels*, Indianapolis, IN, 21 October 1997, p. 1091.
7 **Cyre, J. P.** *Concepts for improving the fatigue resistance of thermite rail welds*. MS Thesis, University of Illinois at Urbana-Champaign, 2002.
8 **Ross, E. T.** *A statistical study of improved thermite rail welds*. MS Thesis, University of Illinois at Urbana-Champaign, 2004.
9 **Oderio, J. A.** *A metallurgical study of the detail fracture in thermite-welded railroad rails*. MS Thesis, University of Illinois at Urbana-Champaign, 1992.
10 **Fry, G. T., Lawrence, F. V.,** and **Robinson, A. R.** Model for fatigue defect nucleation in thermite rail welds. *Fatigue Fract. Eng. Mater. Struct.*, 1996, **19**(6) 655.
11 **Chen, Y., Lawrence, F. V., Barkan, C. P. L.,** and **Dantzig, J. A.** Weld defect formation in rail thermite welds. *Proc. IMechE, Part F: J. Rail and Rapid Transit*, 2006, **220**(F4), 373–384. (This paper.)
12 **Kubo, K.** and **Pehlke, R. D.** Mathematical modeling of porosity formation in solidification. *Metall. Trans. B*, 1985, **16B**, 359.
13 **Overfelt, T.** Manufacturing significance of solidification modeling. *J. Metals*, 1992, **44**(6), 17.
14 **Pellini, W. S.** Factors which determine riser adequacy and feeding range. *Trans. Am. Foundry Soc.*, 1953, **61**, 61.
15 **Niyama, E., Uchida, T., Morikawa, M.,** and **Saito, S.** Predicting shrinkage in large steel castings from temperature gradient calculations. *AFS Int. Casting Metals J.*, 1981, **6**, 16.
16 **Sigworth, G. K.** and **Wang, C.** Mechanisms of porosity formation during solidification: a theoretical analysis. *Metall. Trans. B*, 1993, **24B**, 349.
17 **Niyama, E., Uchida, T., Morikawa, M.,** and **Saito, S.** Method of shrinkage prediction and its application to steel casting practice. *AFS Int. Casting Metals J.*, 1982, **7**(9), 52.
18 **Poirier, D. R., Yeum, K.,** and **Maples, A. L.** A thermodynamic prediction for microporosity formation in aluminum-rich Al-Cu alloys. *Metall. Trans. A*, 1987, **18A**, 1979.
19 **Kurz, W.** and **Fisher, D. J.** *Fundamentals of solidification*, 1986 (Trans Tech Publications, Switzerland).
20 **Carpenter, G. F., Steele, R. K.,** and **Markase, M. J.** Effect of inclusion content on fatigue performance of rail steels. Rail Steels Symposium Proceedings, Montreal, Quebec, Canada, 26–27 October 1992, pp. 49–56.
21 **Barsom, J. M.** and **Imhof, E. J.** Fatigue and fracture behavior of carbon-steel rails. *Rail steels-developments, processing and use* (Eds D. H. Stone and G. G. Knupp), 1978, p. 387 (American Society for Testing and Materials, Philadelphia) ASTM STP 644.

APPENDIX

Notation

d	melt-back depth
d_c	critical melt-back depth
f_E	eutectic fraction
f_L	fraction of interdendritic liquid
G	temperature gradient
M	molecular weight of gas
P_G	gas pressure
P_G^E	gas pressure at eutectic temperature
P_L	liquid pressure
R	cooling rate
T	temperature
T_E	eutectic temperature
V	solidification rate
γ	surface tension
λ_1	primary dendrite arm spacing
ρ_{LE}	mass density of liquid at eutectic temperature
ρ_S'	mass density of solid at eutectic temperature
ϕ	fraction of gas-phase in alloy at eutectic temperature